nature genetics

LETTERS

https://doi.org/10.1038/s41588-018-0053-8

A gain-of-function mutation in the *CLCN2* chloride channel gene causes primary aldosteronism

Fabio L. Fernandes-Rosa[1,2,3,13]*, Georgios Daniil[1,2,13], Ian J. Orozco[4,5,13], Corinna Göppner[4,5], Rami El Zein[1,2], Vandana Jain[6], Sheerazed Boulkroun[1,2], Xavier Jeunemaitre[1,2,3], Laurence Amar[1,2,7], Hervé Lefebvre[8,9,10], Thomas Schwarzmayr[11], Tim M. Strom[11,12], Thomas J. Jentsch[4,5]* and Maria-Christina Zennaro[1,2,3]*

Primary aldosteronism is the most common and curable form of secondary arterial hypertension. We performed whole-exome sequencing in patients with early-onset primary aldosteronism and identified a de novo heterozygous c.71G>A/p.Gly24Asp mutation in the *CLCN2* gene, encoding the voltage-gated ClC-2 chloride channel[1], in a patient diagnosed at 9 years of age. Patch-clamp analysis of glomerulosa cells of mouse adrenal gland slices showed hyperpolarization-activated Cl^- currents that were abolished in *Clcn2*$^{-/-}$ mice. The p.Gly24Asp variant, located in a well-conserved 'inactivation domain'[2,3], abolished the voltage- and time-dependent gating of ClC-2 and strongly increased Cl^- conductance at resting potentials. Expression of ClC-2^{Asp24} in adrenocortical cells increased expression of aldosterone synthase and aldosterone production. Our data indicate that *CLCN2* mutations cause primary aldosteronism. They highlight the important role of chloride in aldosterone biosynthesis and identify ClC-2 as the foremost chloride conductor of resting glomerulosa cells.

Arterial hypertension is a major cardiovascular risk factor[4]. Primary aldosteronism is the most common and curable form of secondary arterial hypertension, with an estimated prevalence of ~10% in referred patients and 4% in primary care[5], and a prevalence of up to 20% in patients with resistant hypertension[6]. Primary aldosteronism results from autonomous aldosterone production in the adrenal cortex[7], caused in most cases by a unilateral aldosterone-producing adenoma or bilateral adrenal hyperplasia (BAH). It is diagnosed on the basis of hypertension associated with an increased aldosterone-to-renin ratio and often hypokalemia[8]. In comparison to essential hypertension, increased aldosterone levels in primary aldosteronism are associated with increased cardiovascular risk, in particular for coronary artery disease, heart failure, renal damage, and stroke[9,10].

Gain-of-function mutations in different genes, encoding cation channels (*KCNJ5*[11], *CACNA1D*[12,13], and *CACNA1H*[14,15]) and ATPases (*ATP1A1* and *ATP2B3*[12,16]), regulating intracellular ion homeostasis and plasma membrane potential, have been described in aldosterone-producing adenoma and familial forms of primary aldosteronism, but the pathophysiology of many cases is still unknown.

We performed whole-exome sequencing on germline DNA from 12 patients with young-onset hypertension and hyperaldosteronism diagnosed before 25 years of age. Two index cases were investigated together with their parents and unaffected sibling to search for de novo variants. A de novo germline *CLCN2* variant, c.71G>A (NM_004366; p.Gly24Asp), was identified in subject K1011-1, but not in her asymptomatic parents (K1011-3 and K1011-4) and sibling (K1011-2; Fig. 1a,b and Table 1). The variant was absent from more than 120,000 alleles in the Exome Aggregation Consortium (ExAC) database and in our in-house database. We did not find additional *CLCN2* variants among the other 11 investigated individuals. *CLCN2* encodes the chloride channel ClC-2. The variant p.Gly24Asp is located in its N-terminal cytoplasmic domain (Fig. 1c,d). Gly24 is highly conserved in ClC-2 from species as distant as zebrafish and *Xenopus tropicalis* (Fig. 1c).

The patient carrying the *CLCN2* variant encoding p.Gly24Asp is a 9-year-old girl who presented with severe headache and vomiting lasting for 1 year (Table 1). The child was developmentally normal, first born to a non-consanguineous couple. There was a history of mild hypertension in the maternal grandmother and granduncle. Blood pressure was 172/100 mm Hg, and heart rate was 120 beats/min. The rest of the examination was normal. Her work-up showed persistent hypokalemia (serum K^+ ranging from 1.8 to 2.4 meq/L), elevated serum aldosterone (868.1 pg/ml, reference range 12–340 pg/ml), and suppressed plasma renin activity (0.11 ng/ml/h, reference range 1.9 to 6.0 ng/ml/h in an upright posture), suggestive of primary aldosteronism. Abdominal computed tomography (CT) scans showed no adrenal abnormalities. Other parameters including 24-h urinary vanillylmandelic acid and serum cortisol were normal. Hypertension was initially managed with amlodipin, enalapril, and atenolol. Once the diagnosis of primary aldosteronism was made, spironolactone was added, enalapril was stopped, and the doses of amlodipin and atenolol were reduced. Serum K^+ normalized. A positive glucocorticoid suppression test (with aldosterone at 949.3 pg/ml at baseline and 56.9 pg/ml after oral administration of 0.5 mg of dexamethasone every 6 h for 48 h) suggested the possibility of glucocorticoid-remediable aldosteronism (GRA), a rare familial

[1]INSERM, UMRS 970, Paris Cardiovascular Research Center, Paris, France. [2]Université Paris Descartes, Sorbonne Paris Cité, Paris, France. [3]Assistance Publique–Hôpitaux de Paris, Hôpital Européen Georges Pompidou, Service de Génétique, Paris, France. [4]Leibniz-Forschungsinstitut für Molekulare Pharmakologie (FMP), Berlin, Germany. [5]Max Delbrück Centrum für Molekulare Medizin (MDC), Berlin, Germany. [6]Division of Pediatric Endocrinology, Department of Pediatrics, All India Institute of Medical Sciences, New Delhi, India. [7]Assistance Publique–Hôpitaux de Paris, Hôpital Européen Georges Pompidou, Unité Hypertension Artérielle, Paris, France. [8]Normandie Université, UNIROUEN, Rouen, France. [9]INSERM, DC2N, Rouen, France. [10]Department of Endocrinology, Diabetes and Metabolic Diseases, University Hospital of Rouen, Rouen, France. [11]Institute of Human Genetics, Helmholtz Zentrum München, Neuherberg, Germany. [12]Institute of Human Genetics, Technische Universität München, Munich, Germany. [13]These authors contributed equally: Fabio L. Fernandes-Rosa, Georgios Daniil and Ian J. Orozco. *e-mail: fabio.fernandes-rosa@inserm.fr; jentsch@fmp-berlin.de; maria-christina.zennaro@inserm.fr

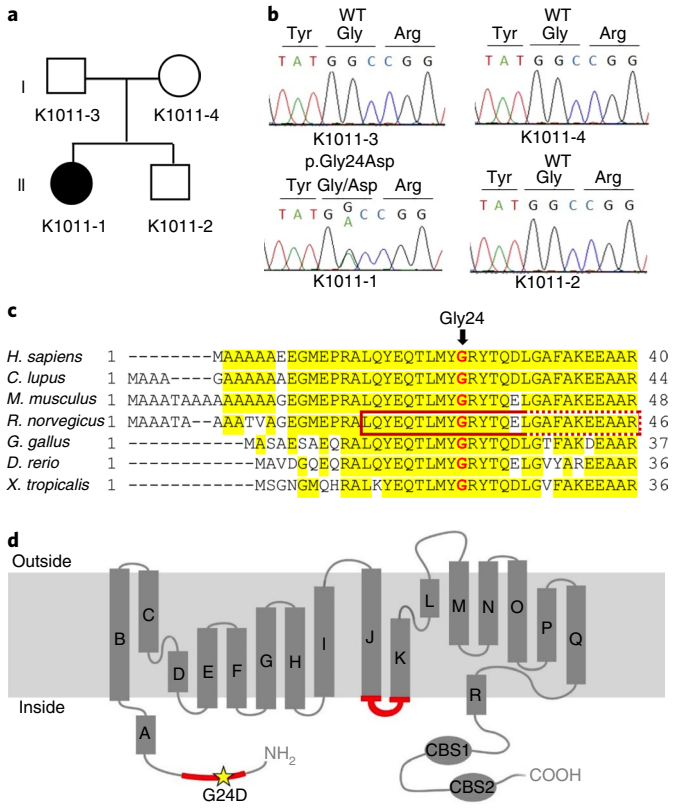

Table 1 | Clinical and biological characteristics of individuals carrying *CLCN2* variants

	K1011-1	K963-1	K1044-1
Sex	F	F	F
Age at HTN dg (years)	9	19	29
Age at primary aldosteronism dg (years)	9	27	48
SBP at primary aldosteronism dg (mm Hg)	172	139	173
DBP at primary aldosteronism dg (mm Hg)	100	90	114
Lowest plasma K^+ (mmol/L)	1.8	2.9	2.5
Urinary aldosterone (nmol/24 h)	ND	60	ND
Plasma aldosterone (pmol/L)	2,406	927	1,061
Plasma renin (mU/L)	0.9	1.9	<1
ARR (pmol/mU)	481.2	185.4	212.2
Adrenal abnormalities on imaging	No	No	No
Lateralization at AVS	ND	No	No

Hormonal data were obtained at diagnosis of primary aldosteronism. For comparison within this table, plasma aldosterone levels for patient K1011-1 were converted to pmol/L and plasma renin activity was converted to plasma renin concentration. For ARR calculation, renin values <5 were transformed to 5. The conversion factor used for plasma aldosterone was 1 ng/L = 2.77 pmol/L, and the conversion factor used for plasma renin was 1 ng/ml/h = 8.2 mU/L. dg, diagnosis; HTN, hypertension; SBP, systolic blood pressure; DBP, diastolic blood pressure; ARR, aldosterone-to-renin ratio; ND, not determined; AVS, adrenal venous sampling

Fig. 1 | A *CLCN2* variant identified in a patient with early-onset primary aldosteronism. a, Pedigree of kindred K1011. The subject with primary aldosteronism is shown with a filled symbol, and non-affected subjects are shown with unfilled symbols. **b**, Sanger sequencing chromatograms showing the wild-type *CLCN2* sequence of the unaffected parents (K1011-3 and K1011-4) and brother (K1011-2) and the *CLCN2* variant c.71G>A (p.Gly24Asp) identified in the patient with early-onset primary aldosteronism (K1011-1). **c**, Alignment and conservation of residues encoded by *CLCN2* orthologs. The red box indicates the N-terminal inactivation domain of ClC-2. Several deletions and mutations mapping to this region of rat ClC-2 lead to constitutively open ClC-2 channels (solid line) or partially open channels (dashed line)[3]. Residues that are conserved among more than three sequences are highlighted in yellow. **d**, Position of the disease-causing p.Gly24Asp variant in the ClC-2 protein (schematic transmembrane topology drawing modified from ref. [36]). Inactivation domains previously identified by structure–function analysis in the N terminus[3] and an intracellular loop[2] of ClC-2 are shown in red. Several point mutations and deletions affecting these domains open the ClC-2 channel[2,3] similarly to the p.Gly24Asp substitution described here. CBS1 and CBS2 are cystathionine-β-synthase domains that can affect gating of ClC channels[23].

form of hyperaldosteronism[17]. However, genetic analysis for a chimeric *CYP11B1-CYP11B2* gene was negative. The child's hypertension has been well controlled over 18 months with prednisolone at 5 mg/m²/d, spironolactone, and amlodipin. On treatment, her serum aldosterone and plasma renin levels are 421 pg/ml (reference range 25 to 392 pg/ml) and 8.22 µU/ml (4.4 to 46.1 µU/ml), respectively. After exclusion of GRA by genetic testing, prednisolone treatment was stopped.

Cl^- conductance can regulate the excitability of neuronal, muscle, and endocrine cells[18–21]. In zona glomerulosa cells, adrenocorticotropic hormone (ACTH)-activated Cl^- currents have been described[22], but their outward rectification sets them apart from hyperpolarization-activated ClC-2 currents. ClC-2 is expressed in almost all tissues[1] and may have roles in ion homeostasis and transepithelial transport[23]. *Clcn2*$^{-/-}$ mice display early postnatal retinal and testicular degeneration[24] as well as leukodystrophy[25,26]; in humans, *CLCN2* loss-of-function mutations result in leukodystrophy[27] that may be associated with azoospermia[28]. These phenotypes have been ascribed to a role for ClC-2 in extracellular ion homeostasis[24,25].

Data retrieved from a transcriptome analysis including 11 human adrenal glands[29] showed high expression of *CLCN2* in human adrenal cortex (Supplementary Table 1). In mice, western blots showed similar expression of ClC-2 in whole adrenal gland as in brain (Fig. 2a), which expresses substantial, physiologically important amounts of ClC-2[25]. Patch-clamp analysis of glomerulosa cells in situ showed typical hyperpolarization-activated currents in wild-type mice, but not in *Clcn2*$^{-/-}$ mice (Fig. 2b,c). The magnitude of these currents was similar to those observed in Bergmann glia, which prominently express ClC-2[26]. The almost complete absence of Cl^- currents in *Clcn2*$^{-/-}$ cells demonstrates that under resting conditions ClC-2 mediates the bulk of glomerulosa cell Cl^- currents.

The ClC-2 p.Gly24Asp variant is located in a highly conserved inactivation domain[2,3] of the channel. Deletions and point mutations mapping to this region and to an intracellular loop[2] (highlighted in Fig. 1c,d) lead to 'open' ClC-2 channels that have lost their sensitivity to voltage, cell swelling, or external pH[2,3]. Likewise, insertion of the p.Gly24Asp variant drastically changed voltage-dependent gating of ClC-2 (Fig. 2d,e,h) and dramatically increased current amplitudes when the human protein was expressed in *Xenopus laevis* oocytes (Fig. 2d–g). When measured at –80 mV, the approximate resting potential of glomerulosa cells[30], current amplitudes from the mutant channel were much larger than those for the wild-type channel (Fig. 2d–f). Linear, ohmic currents like those of the mutant channel might be due to unspecific electrical leaks; however, the currents of both wild-type and mutant ClC-2 were markedly reduced when extracellular chloride was replaced by iodide (Fig. 2d–f), in agreement with the $Cl^- > I^-$ selectivity of ClC channels in general[23] and ClC-2 in particular[1]. The activation of ClC-2 by an acidic

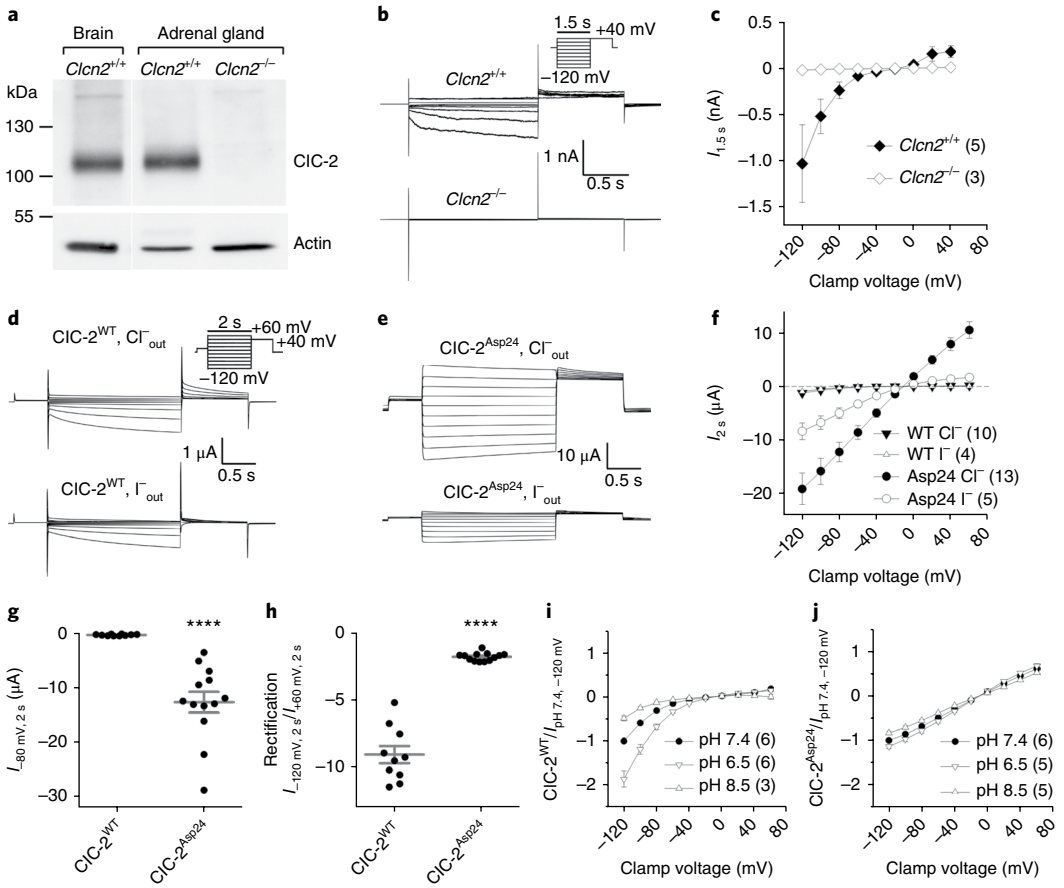

Fig. 2 | ClC-2 expression in mouse adrenal glands and electrophysiological analyses of wild-type and mutant channels. a, ClC-2 immunoblot of brain and adrenal glands from *Clcn2*$^{+/+}$ and *Clcn2*$^{-/-}$ mice. All lanes are from the same blot, which was cut where indicated. Similar amounts of protein were loaded with actin serving as a loading control. This blot is representative of three independent experiments. **b**, Representative whole-cell chloride current traces of mouse zona glomerulosa cells from *Clcn2*$^{+/+}$ (top) and *Clcn2*$^{-/-}$ (bottom) adrenal slices using voltage steps as indicated above. **c**, Mean ± s.e.m. currents measured after 1.5 s from the experiments in **b** plotted as a function of clamp voltage. The number of cells analyzed is given in parentheses. **d**,**e**, Representative chloride current traces measured by two-electrode voltage-clamp from *Xenopus* oocytes injected with either human ClC-2^{WT} (**d**) or ClC-2^{Asp24} (**e**) cRNA, using the protocol shown in **d**. For some measurements (below), extracellular chloride was replaced with iodide. **f**, Mean ± s.e.m. currents measured in **d** and **e** plotted as a function of voltage. The number of cells analyzed is given in parentheses. **g**,**h**, Summary of Cl$^-$ currents at −80 mV ($I_{-80\,mV}$) (**g**) and current ratios ($I_{-120\,mV}/I_{+60\,mV}$) as a measure of rectification (**h**) (always measured at 2 s) for panels **d**–**f**. ****$P < 0.0001$, Mann–Whitney two-tailed test. **i**,**j**, Effect of external pH on currents mediated by ClC-2^{WT} (**i**) and ClC-2^{Asp24} (**j**) in *Xenopus* oocytes. Currents were normalized to mean currents from the respective construct measured after 2 s at −120 mV and at pH 7.4. The number of oocytes analyzed is given in parentheses; error bars, s.e.m.

extracellular pH can be almost abolished by mutations mapping to the inactivation domain[2]. Likewise, the ClC-2^{Asp24} mutant had largely reduced pH sensitivity (Fig. 2i,j and Supplementary Fig. 1). In conclusion, the p.Gly24Asp variant results in a strong gain of function, in line with the dominant disease phenotype of the mutation that is present in the heterozygous state. It also suggests a pathophysiological mechanism in which a strong increase in Cl$^-$ currents may depolarize glomerulosa cells, thereby opening voltage-gated Ca^{2+} channels and activating transcriptional programs via an increase in cytosolic Ca^{2+}.

Expression of the mutant ClC-2^{Asp24} channel in human adrenocortical H295R-S2 cells and, conversely, knockdown of ClC-2 by shRNA significantly affected aldosterone production and expression of steroidogenic enzymes. Despite similar expression of ClC-2 in H295R-S2 cells stably transfected to express ClC-2^{Asp24} and wild-type ClC-2 (ClC-2^{WT}) (Fig. 3a,b), aldosterone synthase expression (Fig. 3a,c) and aldosterone production (Fig. 3d,e) were significantly increased in ClC-2^{Asp24}-expressing cells. Stimulation with angiotensin II (Ang II; 10 nM) or K^+ (12 mM) increased aldosterone production in cells expressing ClC-2^{WT} (Fig. 3e). A further increase was observed in cells expressing ClC-2^{Asp24} after Ang II stimulation, but not after K^+ stimulation (Fig. 3e). Nevertheless, also after stimulation, aldosterone production in cells expressing ClC-2^{Asp24} was significantly higher than in cells expressing ClC-2^{WT} (Fig. 3e). Infection of H295R-S2 cells with shRNA constructs targeting ClC-2 reduced *CLCN2* expression by ~50% (Supplementary Fig. 2a) as compared with a scrambled shRNA and significantly reduced aldosterone production, both at baseline and after stimulation (Supplementary Fig. 2b), suggesting that even ClC-2^{WT} currents, although much smaller than currents from the ClC-2^{Asp24} mutant, increase the excitability of H295R-S2 adrenocortical cells. These changes were paralleled in both models by concomitant modifications of the expression of steroidogenic genes. An increase in the mRNA expression of *CYP11B2* (encoding aldosterone synthase; Fig. 3f), *STAR* (encoding the steroidogenic acute regulatory protein; Fig. 3g), and *CYP21A2* (encoding steroid 21-hydroxylase; Fig. 3h) was observed in ClC-2^{Asp24}- as compared with ClC-2^{WT}-overexpressing cells under basal conditions. Ang II increased expression of *STAR* and *CYP11B2*, while K^+ stimulation increased mRNA expression of *CYP11B2*. Conversely, knockdown of ClC-2 led to a decrease in

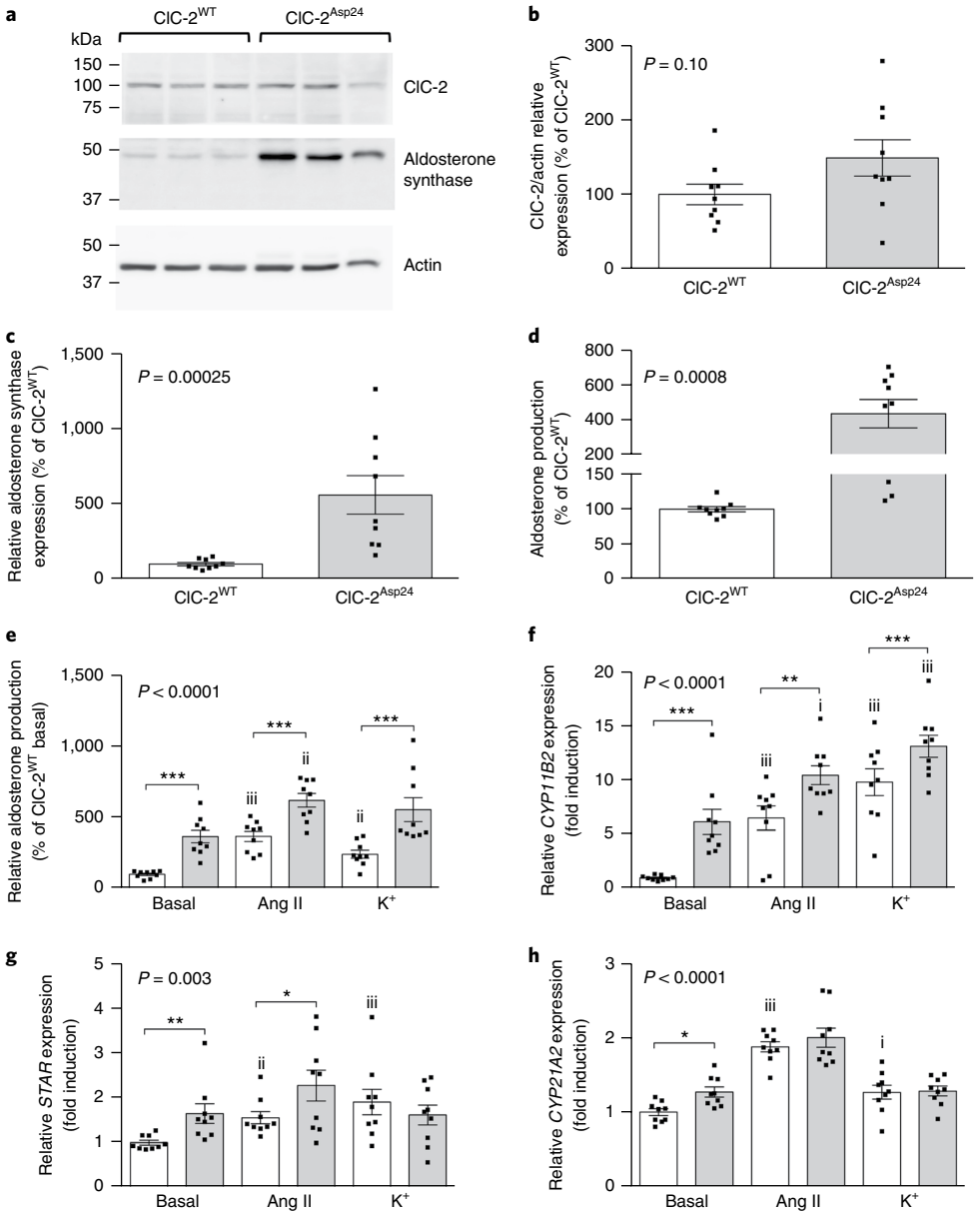

Fig. 3 | Effect of ClC-2^{WT} and mutant ClC-2^{Asp24} channels on aldosterone production and expression of genes and proteins involved in aldosterone biosynthesis. a, Western blots for ClC-2 and aldosterone synthase of H295R-S2 cells stably transfected to express ClC-2^{WT} or mutant ClC-2^{Asp24}. These blots are representative of three independent experiments, with actin serving as a loading control. **b**, Quantification of ClC-2 protein levels in ClC-2^{WT} and ClC-2^{Asp24} H295R-S2 cells (*t* test, $P=0.10$, $F=3.19$). **c**, Quantification of aldosterone synthase expression in ClC-2^{WT} and ClC-2^{Asp24} H295R-S2 cells (*t* test, $P=0.0025$, $F=136$). **d**, Basal aldosterone production by H295R-S2 cells transfected to express ClC-2^{WT} or mutant ClC-2^{Asp24} (*t* test, $P=0.0008$, $F=142$). **e**, Basal and stimulated aldosterone production by H295R-S2 cells transfected to express ClC-2^{WT} (open bars) or mutant ClC-2^{Asp24} (filled bars) (one-way ANOVA, $P<0.0001$, $F=23.46$). **f**–**h**, Basal and stimulated mRNA expression of *CYP11B2* (one-way ANOVA, $P<0.001$, $F=18.39$) (**f**), *STAR* (Kruskal–Wallis, $P=0.0033$) (**g**), and *CYP21A2* (one-way ANOVA, $P<0.0001$, $F=23.27$) (**h**) in H295R-S2 cells transfected to express ClC-2^{WT} (open bars) or mutant ClC-2^{Asp24} (filled bars). Quantifications of protein expression (using actin as a loading control) and aldosterone production are presented as the percentage of the value for ClC-2^{WT}-expressing cells under basal conditions, and the results of mRNA expression are presented as fold induction relative to ClC-2^{WT}-expressing cells under basal conditions. Values of all experiments are presented as the means ± s.e.m. of three independent experiments performed in experimental triplicate ($n=9$) for each condition. $^*P<0.05$; $^{**}P<0.01$; $^{***}P<0.001$; i, $P<0.05$ for the stimulated versus basal condition; ii, $P<0.01$ for the stimulated versus basal condition; iii, $P<0.001$ for the stimulated versus basal condition.

CYP11B2 expression under all conditions (Supplementary Fig. 2c). These data further support the notion that a gain-of-function *CLCN2* mutation may depolarize the cell, activate the steroidogenic pathway, and increase aldosterone production. While knockdown of ClC-2 influences aldosterone production in H295R-S2 cells, which have a resting potential of about −65 mV (Fig. 4a,b), this may not be the case in native glomerulosa cells. Because their membrane voltage (V_m) is close to the K^+ equilibrium potential[30], they are unlikely to markedly hyperpolarize upon loss of ClC-2. No changes in blood pressure have been reported for mice or patients lacking ClC-2[24,25,27], but this issue has not been investigated in detail.

We next explored the effect of the ClC-2 p.Gly24Asp variant on membrane potential and calcium influx through voltage-gated calcium channels. These studies were performed with the perforated

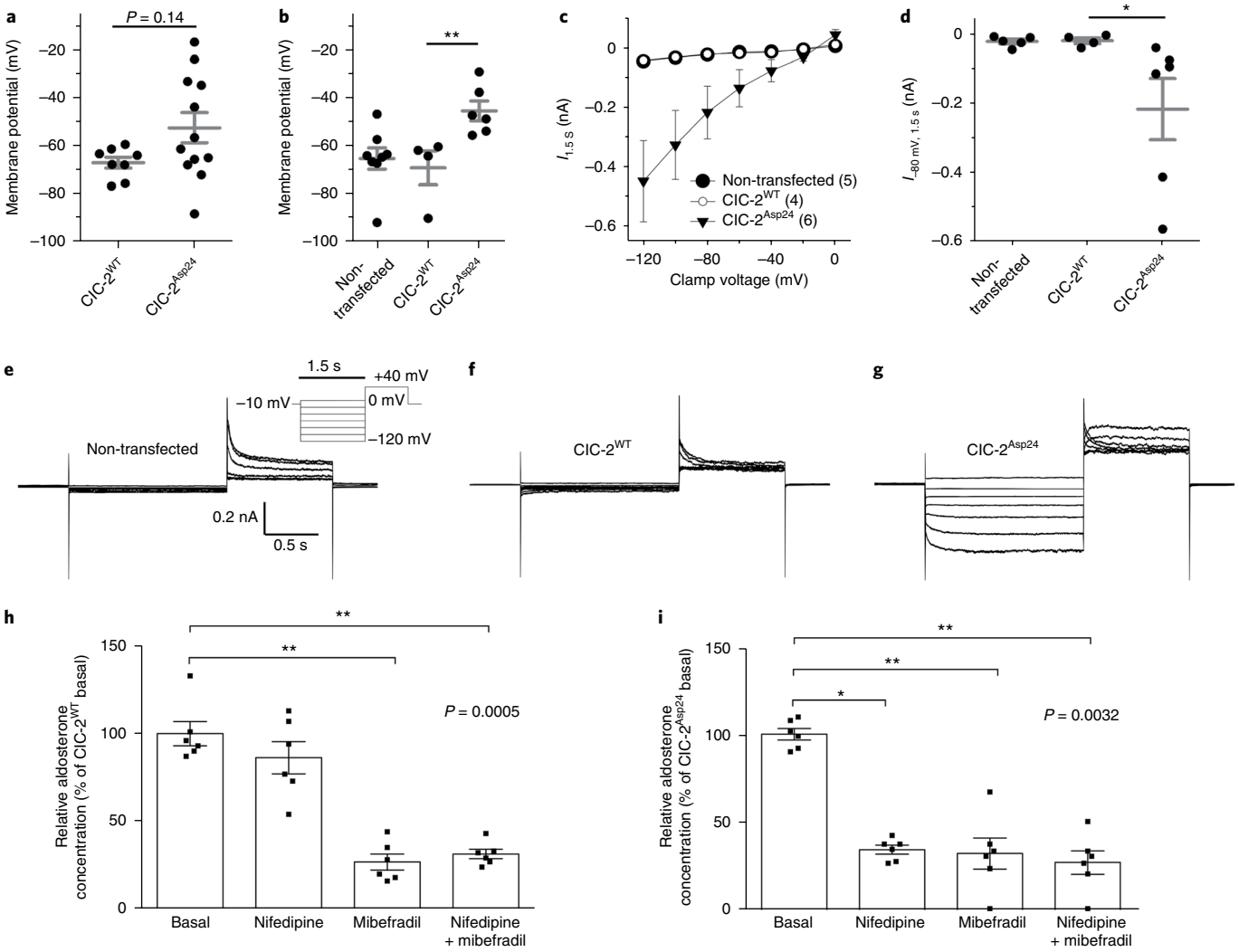

Fig. 4 | Functional impact of the ClC-2^{Asp24} variant. a–g, Effect on membrane potential (V_m) and plasma membrane anion currents in H295R-S2 cells. **a**, Resting membrane potential of the ClC-2^{WT} and ClC-2^{Asp24} channels in the stably transfected H295R-S2 cells that were used to determine aldosterone secretion. Note the strong mean depolarization (ClC-2^{WT}, −67 ± 2 mV (n = 8); ClC-2^{Asp24}, −52 ± 6 mV (n = 12)), which, however, was not significant (two-tailed Mann–Whitney, P = 0.14) owing to large variability in V_m for ClC-2^{Asp24}-expressing cells that were not clonally selected. **b**, Similarly determined values of V_m for non-transfected and transiently transfected H295R-S2 cells (non-transfected, −65 ± 4 mV (n = 8); ClC-2^{WT}, −69 ± 7 mV (n = 4); ClC-2^{Asp24}, −46 ± 4 mV (n = 6); **P = 0.0095, two-tailed Mann–Whitney test). **c**,**d**, Corresponding plasma membrane currents measured after 1.5 s under conditions eliminating cation inward currents plotted as a function of voltage (**c**) or as individual values at the physiological V_m of glomerulosa cells (**d**). The number of cells analyzed is given in parentheses. *P = 0.019, two-tailed Mann–Whitney test. **e**–**g**, Corresponding averaged current traces with 20-mV voltage steps between 0 and −120 mV for non-transfected cells (**e**) and cells expressing ClC-2^{WT} (**f**) and ClC-2^{Asp24} (**g**). **h**,**i**, Effect of calcium channel blockers on aldosterone production in H295R-S2 cells expressing ClC-2^{WT} (Kruskal–Wallis, P = 0.0005) (**h**) and ClC-2^{Asp24} (Kruskal–Wallis, P = 0.0032) (**i**). Values represent the means ± s.e.m. of two independent experiments performed in experimental triplicate (n = 6) for each condition. Dunn's post test for the treated versus basal condition: *P < 0.05, **P < 0.01.

patch-clamp technique, which does not disturb the intracellular chloride concentration and is required to see the full effect of inactivation domain[2,3] mutations[31,32]. In the stably transfected H295R-S2 cells used to investigate steroidogenesis (Fig. 3), there was a trend toward V_m being depolarized in ClC-2^{Asp24}- as compared to ClC-2^{WT}-overexpressing cells (mean values of roughly −52 and −67 mV, respectively) (Fig. 4a). However, because these cell lines were not clonal, the variability was large and the difference was not statistically significant.

We therefore resorted to transient transfection of H295R-S2 cells, which allowed us to select ClC-2-expressing cells by fluorescence of cotransfected GFP (Fig. 4b–g). Although these cells express ClC-2 less efficiently than *Xenopus* oocytes (compare Figs. 4f and 2d) and HEK cells[31,32], ClC-2^{Asp24}-expressing cells displayed robust Cl^- currents that lacked strong voltage dependence (Fig. 4c–g). The observed increase in currents may reflect increases in both the currents for individual channels and the number of channels; both must be considered when analyzing the pathogenic effects of ion channel mutants. This increase in currents correlated with a strong depolarization from V_m = −69 ± 7 mV in ClC-2^{WT}-expressing cells to −46 ± 4 mV in ClC-2^{Asp24}-expressing cells (Fig. 4b), indicating that chloride concentration in H295R-S2 cells is higher than predicted from the electrochemical equilibrium. This depolarization may open voltage-dependent calcium channels. Indeed, nifedipine (an L-type calcium channel blocker) and/or mibefradil (a T-type calcium channel blocker) strongly reduced aldosterone production in cells expressing the ClC-2^{Asp24} mutant (Fig. 4i). The involvement of L-type calcium channels appeared to be larger in ClC-2^{Asp24}-expressing

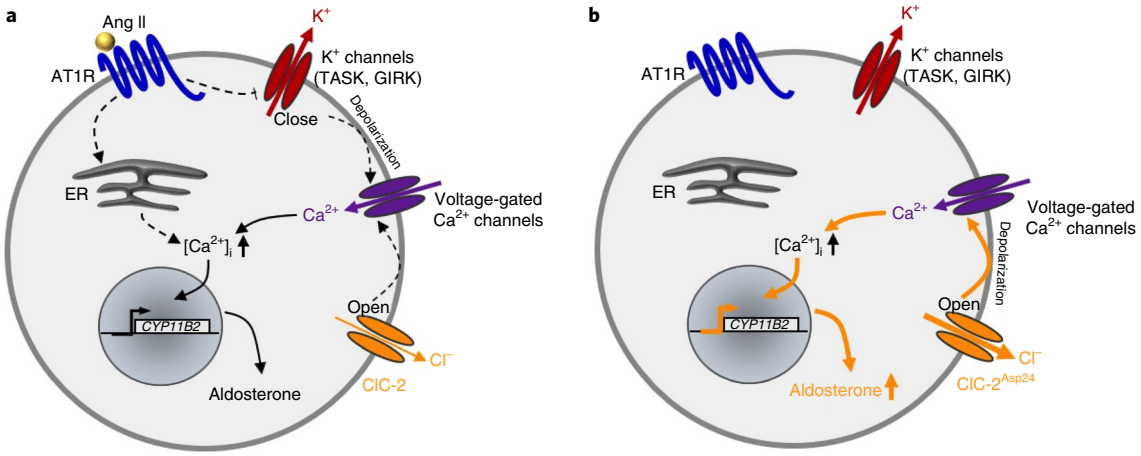

Fig. 5 | Proposed model for autonomous aldosterone secretion in adrenal zona glomerulosa cells with the ClC-2^{Asp24} mutant. a, In unstimulated conditions, the zona glomerulosa cell membrane potential closely follows the potassium resting potential at approximately −80 mV. Increasing extracellular K^+ concentration, or inhibition of K^+ channels by Ang II through its receptor (AT1R), leads to cell membrane depolarization, opening of voltage-gated Ca^{2+} channels, and increased intracellular calcium concentrations, the major trigger for aldosterone biosynthesis. Binding of Ang II to AT1R also leads to $G_{\alpha q}$-mediated signaling and IP_3-mediated release of Ca^{2+} from the endoplasmic reticulum (ER). **b**, The ClC-2 p.Gly24Asp variant abolishes the voltage-dependent gating of ClC-2. The resulting pronounced increase in Cl^- currents at resting potentials is proposed to result in cell depolarization, opening of voltage-gated Ca^{2+} channels, stimulation of Ca^{2+} signaling, and, ultimately, increased expression of steroidogenic genes and aldosterone production. $[Ca^{2+}]_i$, intracellular calcium concentration.

cells (Fig. 4h), possibly because of the depolarized plasma membrane potential of these cells, which is required to open L-type calcium channels[33]. However, we cannot exclude the possibility that nifedipine acted partially through T-type calcium channels, which are also blocked by this compound at depolarized voltages[34].

To investigate whether the *CLCN2* mutation encoding p.Gly24Asp could be involved in other forms of primary aldosteronism, we sequenced exon 2 of *CLCN2* in 100 patients with BAH. While the *CLCN2* mutation encoding p.Gly24Asp was not identified among these subjects, we found two rare *CLCN2* variants, c.197G>A (p.Arg66Gln, rs755883734) and c.143C>G (p.Pro48Arg, rs115661422) in two subjects (Supplementary Fig. 3). The minor allele frequencies of these variants were very low in the ExAC database (*CLCN2* p.Arg66Gln, 0.00003; *CLCN2* p.Pro48Arg, 0.0017). Both variants failed to significantly change ClC-2 currents in *Xenopus* oocytes in which the mutant proteins were heterologously expressed (Supplementary Fig. 4), in spite of a previously described[35] moderate reduction in ClC-2^{Arg48} current amplitudes. Nonetheless, it is noteworthy that the two patients were diagnosed with hypertension at a young age, at 29 and 19 years, respectively (Table 1), and in both cases during pregnancy. Finally, sequencing the *CLCN2* exons encoding the N-terminal domain (exons 1 and 2) and the loop between helices J and K (exon 10), corresponding to the ClC-2 inactivation domains[2,3], in 20 additional patients with hypertension before 20 years of age did not identify additional mutations. Among these patients, nine had a history of hypertension before the age of 15 years (one before 10 years), indicating that *CLCN2* mutations might underlie forms of primary aldosteronism with very young onset.

In conclusion, we show that a gain-of-function mutation affecting the ClC-2 chloride channel underlies a genetic form of secondary arterial hypertension and identify ClC-2 as the foremost chloride conductor of resting glomerulosa cells. We suggest that increased Cl^- currents induced by the ClC-2 p.Gly24Asp variant could depolarize the zona glomerulosa cell membrane, thereby opening voltage-gated calcium channels that trigger autonomous aldosterone production by increasing intracellular Ca^{2+} concentrations (Fig. 5b, orange arrows). We hypothesize that the increased Cl^- currents may overcome the hyperpolarizing currents of K^+ channels that normally determine the glomerulosa cell resting potential. The inhibition of these potassium channels, for example upon Ang II stimulation, or the depolarizing currents mediated by these channels upon increases in extracellular K^+ are the main mechanisms triggering aldosterone production under physiological conditions (Fig. 5a, dashed black arrows).

Not only mutations mapping to the N-terminal ClC-2 inactivation domain[2,3], like the p.Gly24Asp variant found here, but also those mapping to the cytoplasmic linker between transmembrane helices J and K may cause primary aldosteronism (Fig. 1d). Several point mutations affecting this linker result in constitutively open ClC-2 channels[2]. We propose both regions as potential hotspots for mutations causing primary aldosteronism. The discovery that a chloride channel is involved in primary aldosteronism opens new and unexpected perspectives for the pathogenesis and treatment of arterial hypertension.

Methods

Methods, including statements of data availability and any associated accession codes and references, are available at https://doi.org/10.1038/s41588-018-0053-8.

Received: 25 July 2017; Accepted: 3 January 2018;
Published online: 5 February 2018

References

1. Thiemann, A., Gründer, S., Pusch, M. & Jentsch, T. J. A chloride channel widely expressed in epithelial and non-epithelial cells. *Nature* **356**, 57–60 (1992).
2. Jordt, S. E. & Jentsch, T. J. Molecular dissection of gating in the ClC-2 chloride channel. *EMBO J.* **16**, 1582–1592 (1997).
3. Gründer, S., Thiemann, A., Pusch, M. & Jentsch, T. J. Regions involved in the opening of CIC-2 chloride channel by voltage and cell volume. *Nature* **360**, 759–762 (1992).
4. NCD Risk Factor Collaboration (NCD-RisC). Worldwide trends in blood pressure from 1975 to 2015: a pooled analysis of 1479 population-based measurement studies with 19·1 million participants. *Lancet* **389**, 37–55 (2017).
5. Hannemann, A. & Wallaschofski, H. Prevalence of primary aldosteronism in patient's cohorts and in population-based studies—a review of the current literature. *Horm. Metab. Res.* **44**, 157–162 (2012).
6. Calhoun, D. A. Hyperaldosteronism as a common cause of resistant hypertension. *Annu. Rev. Med.* **64**, 233–247 (2013).

7. Zennaro, M. C., Boulkroun, S. & Fernandes-Rosa, F. Genetic causes of functional adrenocortical adenomas. *Endocr. Rev.* **38**, 516–537 (2017).
8. Funder, J. W. et al. The management of primary aldosteronism: case detection, diagnosis, and treatment: an Endocrine Society Clinical Practice Guideline. *J. Clin. Endocrinol. Metab.* **101**, 1889–1916 (2016).
9. Savard, S., Amar, L., Plouin, P. F. & Steichen, O. Cardiovascular complications associated with primary aldosteronism: a controlled cross-sectional study. *Hypertension* **62**, 331–336 (2013).
10. Rossi, G. P. et al. A prospective study of the prevalence of primary aldosteronism in 1,125 hypertensive patients. *J. Am. Coll. Cardiol.* **48**, 2293–2300 (2006).
11. Choi, M. et al. K^+ channel mutations in adrenal aldosterone-producing adenomas and hereditary hypertension. *Science* **331**, 768–772 (2011).
12. Azizan, E. A. et al. Somatic mutations in *ATP1A1* and *CACNA1D* underlie a common subtype of adrenal hypertension. *Nat. Genet.* **45**, 1055–1060 (2013).
13. Scholl, U. I. et al. Somatic and germline *CACNA1D* calcium channel mutations in aldosterone-producing adenomas and primary aldosteronism. *Nat. Genet.* **45**, 1050–1054 (2013).
14. Scholl, U. I. et al. Recurrent gain of function mutation in calcium channel *CACNA1H* causes early-onset hypertension with primary aldosteronism. *eLife* **4**, e06315 (2015).
15. Daniil, G. et al. *CACNA1H* mutations are associated with different forms of primary aldosteronism. *EBioMedicine* **13**, 225–236 (2016).
16. Beuschlein, F. et al. Somatic mutations in *ATP1A1* and *ATP2B3* lead to aldosterone-producing adenomas and secondary hypertension. *Nat. Genet.* **45**, 440–444 (2013).
17. Lifton, R. P. et al. A chimaeric 11β-hydroxylase/aldosterone synthase gene causes glucocorticoid-remediable aldosteronism and human hypertension. *Nature* **355**, 262–265 (1992).
18. Moss, S. J. & Smart, T. G. Constructing inhibitory synapses. *Nat. Rev. Neurosci.* **2**, 240–250 (2001).
19. Rinke, I., Artmann, J. & Stein, V. ClC-2 voltage-gated channels constitute part of the background conductance and assist chloride extrusion. *J. Neurosci.* **30**, 4776–4786 (2010).
20. Koch, M. C. et al. The skeletal muscle chloride channel in dominant and recessive human myotonia. *Science* **257**, 797–800 (1992).
21. Guo, J. H. et al. Glucose-induced electrical activities and insulin secretion in pancreatic islet β-cells are modulated by CFTR. *Nat. Commun.* **5**, 4420 (2014).
22. Chorvátová, A., Gendron, L., Bilodeau, L., Gallo-Payet, N. & Payet, M. D. A Ras-dependent chloride current activated by adrenocorticotropin in rat adrenal zona glomerulosa cells. *Endocrinology* **141**, 684–692 (2000).
23. Jentsch, T. J. Discovery of CLC transport proteins: cloning, structure, function and pathophysiology. *J. Physiol.* **593**, 4091–4109 (2015).
24. Bösl, M. R. et al. Male germ cells and photoreceptors, both dependent on close cell–cell interactions, degenerate upon ClC-2 Cl^- channel disruption. *EMBO J.* **20**, 1289–1299 (2001).
25. Blanz, J. et al. Leukoencephalopathy upon disruption of the chloride channel ClC-2. *J. Neurosci.* **27**, 6581–6589 (2007).
26. Hoegg-Beiler, M. B. et al. Disrupting MLC1 and GlialCAM and ClC-2 interactions in leukodystrophy entails glial chloride channel dysfunction. *Nat. Commun.* **5**, 3475 (2014).
27. Depienne, C. et al. Brain white matter oedema due to ClC-2 chloride channel deficiency: an observational analytical study. *Lancet Neurol.* **12**, 659–668 (2013).
28. Di Bella, D. et al. Subclinical leukodystrophy and infertility in a man with a novel homozygous *CLCN2* mutation. *Neurology* **83**, 1217–1218 (2014).
29. Boulkroun, S. et al. Prevalence, clinical, and molecular correlates of *KCNJ5* mutations in primary aldosteronism. *Hypertension* **59**, 592–598 (2012).
30. Spät, A. & Hunyady, L. Control of aldosterone secretion: a model for convergence in cellular signaling pathways. *Physiol. Rev.* **84**, 489–539 (2004).
31. Varela, D., Niemeyer, M. I., Cid, L. P. & Sepúlveda, F. V. Effect of an N-terminus deletion on voltage-dependent gating of the ClC-2 chloride channel. *J. Physiol.* **544**, 363–372 (2002).
32. Pusch, M., Jordt, S. E., Stein, V. & Jentsch, T. J. Chloride dependence of hyperpolarization-activated chloride channel gates. *J. Physiol.* **515**, 341–353 (1999).
33. Barrett, P. Q. et al. Role of voltage-gated calcium channels in the regulation of aldosterone production from zona glomerulosa cells of the adrenal cortex. *J. Physiol.* **594**, 5851–5860 (2016).
34. Perez-Reyes, E., Van Deusen, A. L. & Vitko, I. Molecular pharmacology of human $Ca_v3.2$ T-type Ca^{2+} channels: block by antihypertensives, antiarrhythmics, and their analogs. *J. Pharmacol. Exp. Ther.* **328**, 621–627 (2009).
35. Paul, J. et al. Alterations in the cytoplasmic domain of CLCN2 result in altered gating kinetics. *Cell. Physiol. Biochem.* **20**, 441–454 (2007).
36. Dutzler, R., Campbell, E. B., Cadene, M., Chait, B. T. & MacKinnon, R. X-ray structure of a ClC chloride channel at 3.0 Å reveals the molecular basis of anion selectivity. *Nature* **415**, 287–294 (2002).

Acknowledgements

This work was funded through institutional support from INSERM and by the Agence Nationale pour la Recherche (ANR-13-ISV1-0006-01), the Fondation pour la Recherche Médicale (DEQ20140329556), the Programme Hospitalier de Recherche Clinique (PHRC grant AOM 06179), and institutional grants from INSERM. The laboratory of M.-C.Z. is also a partner of the H2020 project ENSAT-HT grant number 633983. T.J.J. was supported by institutional funding from the Leibniz and Helmholtz associations, a grant from the BMBF (E-RARE 01GM1403), and the Prix Louis-Jeantet de Médecine.

Author contributions

M.-C.Z., F.L.F.-R., G.D., I.J.O., and T.J.J. designed experiments and wrote the manuscript. T.M.S., M.-C.Z., T.S., and F.L.F.-R. performed and analyzed whole-exome sequencing. M.-C.Z., F.L.F.-R., G.D., R.E.Z., and S.B. performed and analyzed the results of in vitro studies on H295R-S2 cells. I.J.O. performed electrophysiological studies for which the data were analyzed by I.J.O. and T.J.J. C.G. characterized adrenal glands from wild-type and *Clcn2*$^{-/-}$ mice and performed western blots. V.J., X.J., L.A., and H.L. were responsible for patient recruitment, medical care, and clinical data acquisition. All authors revised the manuscript draft. C.G. and R.E.Z. contributed equally to this work.

Competing interests

The authors declare no competing financial interests.

Additional information

Supplementary information accompanies this paper at https://doi.org/10.1038/s41588-018-0053-8.

Reprints and permissions information is available at www.nature.com/reprints.

Correspondence and requests for materials should be addressed to F.L.F. or T.J.J. or M.-C.Z.

Methods

Patients. Patients with primary aldosteronism were recruited within the COMETE (COrtico- et MEdullo-surrénale, les Tumeurs Endocrines) network (COMETE-HEGP protocol, authorization CPP 2012-A00508-35) or in the context of genetic screening for familial hyperaldosteronism at the Genetics Department of the HEGP. Methods for screening and subtype identification of primary aldosteronism were according to the Endocrine Society guidelines[8]. In patients diagnosed with primary aldosteronism, a thin-slice CT scan or magnetic resonance imaging (MRI) of the adrenal and/or an adrenal venous sampling (AVS) was performed to differentiate between unilateral and bilateral aldosterone hypersecretion. All patients gave written informed consent for genetic and clinical investigation. Procedures were in accordance with institutional guidelines (Assistance Publique–Hôpitaux de Paris).

DNA isolation. DNA from peripheral blood leukocytes was extracted using the QIAamp DNA midi kit (Qiagen) or salt extraction.

Whole-exome sequencing and variant detection. Exomes were enriched in solution and indexed with SureSelect XT Human All Exon 50 Mb kits (Agilent). Sequencing was performed as 100-bp paired-end runs on HiSeq 2000 systems (Illumina). Pools of 12 indexed libraries were sequenced on four lanes. Image analysis and base calling were performed using Illumina Real Time Analysis. CASAVA 1·8 was used for demultiplexing. BWA (v 0.5.9) with standard parameters was used for read alignment against human genome assembly hg19 (GRCh37). We performed single-nucleotide variant and small insertion and deletion (indel) calling specifically for the regions targeted by the exome enrichment kit, using SAMtools (v 0.1.18). Subsequently, variant quality was determined using the SAMtools varFilter script. We used default parameters, with the exception of the maximum read depth (-D) and the minimum *P* value for base quality bias (−2), which we set to 9,999 and 1×10^{-400}, respectively. Additionally, we applied a custom script to mark all variants with adjacent bases of low median base quality. All variants were then annotated using custom Perl scripts. Software is available on request (see URLs). Annotation included information about known transcripts (UCSC Known Genes and RefSeq genes), known variants (dbSNP v 135), type of mutation, and—if applicable—amino acid change in the corresponding protein. The annotated variants were then inserted into our in-house database. To reduce false positives, we filtered out variants that were already present in our database, had variant quality less than 40, or failed one of the filters from the filter scripts. We then manually investigated the raw read data of the remaining variants using the Integrative Genomics Viewer (IGV).

Sanger sequencing. *CLCN2* DNA was amplified using the intron-spanning primers described in Supplementary Table 2. PCR was performed on 100 ng of DNA in a final volume of 25 µl containing 0.75 mM $MgCl_2$, 400 nM of each primer, 200 µM deoxynucleotide triphosphate, and 1.25 U Taq DNA Polymerase (Sigma). Cycling conditions for *CLCN2* were as previously described[37] with an annealing temperature of 60 °C. Direct sequencing of PCR products was performed using the ABI Prism Big Dye Terminator v3.1 Cycle Sequencing kit (Applied Biosystems) on an ABI Prism 3700 DNA Analyzer (Applied Biosystems).

Site-directed mutagenesis. The ClC-2^{Asp24} construct was generated by site-directed mutagenesis using the QuikChange II XL site-directed mutagenesis kit (Agilent). The mutation was introduced into the human ClC-2 cDNA fragment inserted into the pFROG expression vector[38], and the presence of the mutation was confirmed by Sanger sequencing.

Western blotting. The membrane fractions of tissue homogenate from brain and adrenal glands of adult *Clcn2*$^{+/+}$ and *Clcn2*$^{-/-}$ mice were isolated and lysed in 50 mM Tris pH 6.8, 140 mM NaCl, 0.5 mM EDTA, and 2% SDS with protease inhibitors (4 mM Pefabloc and Complete EDTA-free protease inhibitor cocktail, Roche). Equal amounts of protein were separated by SDS–PAGE (10% polyacrylamide) and blotted onto nitrocellulose. Rabbit polyclonal antibodies against a modified C-terminal ClC-2 peptide have been described previously[26]. Blots were reprobed with mouse antibody to β-actin (clone AC-74, Sigma, A2228, 1:1,000) as a loading control.

H295R-S2 cells were lysed using RIPA buffer (Bio Basic Canada) with protease and phosphatase inhibitor mini tablets, EDTA free (Thermo Scientific). Proteins were solubilized for 30 min at 4 °C, under end-over-end rotation, and then centrifuged at 13,000 r.p.m. for 15 min at 4 °C. Equal amounts of protein were subjected to 10% SDS–PAGE and transferred onto nitrocellulose. Membranes were blotted with rabbit antibody to ClC-2 (1:500), mouse antibody to aldosterone synthase (1:500, clone CYP11B2-41-13, kindly provided by C. Gomez-Sanchez, University of Mississippi[39]), and mouse antibody to β-actin (A2228, 1:10,000, Sigma).

Electrophysiological recordings. Patch-clamp analysis was performed in adrenal sections from wild-type and *Clcn2*$^{-/-}$ mice[24], similarly to previously described experiments[40]. Bicarbonate-based buffers were used, which were continuously bubbled with 95% O_2 and 5% CO_2. Briefly, adrenal glands were removed and placed into cold low-Ca^{2+} solution composed of (in mM) 140 NaCl, 2 KCl, 26 $NaHCO_3$, 10 glucose, 5 $MgCl_2$, and 0.1 $CaCl_2$, pH 7.4. The adrenal glands, after removal of surrounding fat tissue, were embedded in 3% low-melting agarose, sectioned at 70 µm (Leica, VT1200S), and incubated at room temperature in solution containing (in mM) 140 NaCl, 2 KCl, 26 $NaHCO_3$, 10 glucose, 2 $MgCl_2$, and 2 $CaCl_2$ and adjusted to pH 7.4. After at least 1 h, slices were transferred to a recording chamber and imaged with a 60× objective and DIC optics (Olympus, BX51WI). Cells of the zona glomerulosa were identified by their rosette organization. Electrical signals were acquired at room temperature using a microelectrode amplifier (Multiclamp, 700B) and software (Clampex 10.3, Molecular Devices). As expected, cells when patched with a K^+-based solution displayed spontaneous spiking that could be stimulated with Ang II. For measuring Cl^- currents, patch pipettes were filled with solution containing (in mM) 117.5 $CsMeSO_3$, 17.5 CsCl, 4 NaCl, 10 HEPES, 1 EGTA, and 1 $MgCl_2$, adjusted to pH 7.3, while the bath solution contained (in mM) 117 NMDG-Cl, 23 NMDG-HCO_3, 5 CsCl, 1.3 $MgCl_2$, 9 glucose, and 2 $CaCl_2$, adjusted to pH 7.3. Voltage steps from + 40 to −120 mV from a holding potential of −10 mV were used, with a final 1-s step at +40 mV. Signals were digitized at 10 kHz, filtered at 2 kHz, and stored offline for analysis with Clampfit software 10.4.

For two-electrode voltage-clamp in *Xenopus* oocytes, human wild-type and Gly24Asp ClC-2 cRNAs were prepared from pFROG vectors (Ambion mMESSAGE mMACHINE T7 kit) and injected into *Xenopus* oocytes, at 13.8 ng and 9.2 ng per cell, respectively. Following 2 d of expression at 17 °C, two-electrode voltage-clamp was performed at room temperature using a TurboTEC amplifier (npi electronic) and pClamp software (Molecular Devices) to elicit ClC-2 currents (2-s steps from +60 mV to −120 mV with a final 1-s step at +40 mV) in ND109 solution containing (in mM) 109 NaCl, 2 KCl, 1 $MgCl_2$, 1.8 $CaCl_2$, and 2 HEPES and adjusted to pH 7.4. To test for the typical $Cl^- > I^-$ selectivity of ClC channels, currents were sequentially measured in solutions containing 109 mM Cl^- or 109 mM I^-. To determine the pH sensitivity of currents, ND109 was buffered with 5 mM MES for pH 6.5 and with 5 mM Tris for pH 8.5. Offline analysis was performed with Clampfit software 10.4. Statistical significance was assessed using the Mann–Whitney test (Prism, GraphPad).

For patch-clamp analysis of transiently transfected H295R-S2 cells, cells were seeded at 30% confluence onto coverslips coated with poly-L-lysine (Sigma). Once adhered, they were transfected (X-fect) with bicistronic plasmids encoding emGFP (for identification of transfected cells) and, after an IRES sequence, ClC-2^{WT} or ClC-2^{Asp24}. Cells were measured 12–24 h later. Both transiently and stably transfected cells were measured using a Multiclamp 700B amplifier (Axon Instruments), and gramicidin-perforated patch-clamp was performed so that the intracellular chloride concentration was not disturbed. The tips of patch pipettes were first filled with gramicidin-free internal pipette solution, containing (in mM) 100 $KMeSO_3$, 30 KCl, 4 NaCl, 10 HEPES, 1 $MgCl_2$, 1 EGTA, and 3 MgATP (pH 7.3; 280 mOsm/L), and then backfilled with the same solution containing 25 µg/ml gramicidin. GFP-expressing cells were selected for analysis. Approximately 20 min following tight giga-seal formation, stable membrane potential measurements ($I = 0$ configuration) could be acquired with access resistances of <100 MΩ in bath solution containing (in mM) 140 NaCl, 5 KCl, 10 HEPES, 1.8 $MgCl_2$, and 1.8 $CaCl_2$ (pH 7.4; 300 mOsm/L). When adequate access resistance was attained (<35 MΩ), a Na^+- and K^+-free bath solution containing (in mM) 140 CsCl, 10 HEPES, 1.8 $MgCl_2$, 1.8 $CaCl_2$, and 20 sucrose (pH 7.3; 300 mOsm/L) was perfused to measure anion membrane currents in the voltage-clamp configuration (1-s steps from 0 mV to −120 mV from a holding clamp of −10 mV). Measurements were performed at room temperature (22–24 °C). Data are presented as means ± s.e.m.

Functional studies in H295R-S2 cells. The human adrenocortical carcinoma cell line H295R strain 2 (H295R-S2), kindly provided by W. E. Rainey (University of Michigan)[41], was cultured in DMEM/Eagle's F12 medium (Gibco, Life Technologies) supplemented with 2% Ultroser G (PALL Life Sciences), 1% insulin/transferrin/selenium premix (Gibco, Life Technologies), 10 mM HEPES (Gibco, Life Technologies), and 1% penicillin and streptomycin (Gibco, Life Technologies) and maintained in a 37 °C humidified atmosphere (5% CO_2).

For overexpression experiments, H295R-S2 cells were seeded into tissue culture dishes 100 in groups of 5,000,000 cells per dish and maintained in the conditions described. After 24 h, cells were resuspended in 100 µl of Nucleofector R solution (AMAXA kit, Lonza) and transfected with 3 µg of the ClC-2^{WT} or ClC-2^{Asp24} pFROG construct or a GFP construct, using the electroporation program P-20. To select only stably transfected cells, 48 h after transfection, cells were changed to medium containing 500 µg/ml G418-genetycin (Gibco) and used after all GFP-transfected cells were dead. G418 selection was maintained during all functional studies. For aldosterone measurements and RNA extraction, cells were serum deprived in DMEM/F12 medium containing 0.1% Ultroser G for 24 h and then incubated for another 24 h with fresh medium containing 0.1% Ultroser G with no secretagogue or vehicle (basal), with the secretagogues Ang II (10 nM) or K^+ (12 mM), or with calcium channel blockers nifedipine (L-type calcium channel blocker, 10 µM, Sigma) or mibefradil (T-type calcium channel blocker, 10 µM, Sigma). At the end of the incubation time, supernatant and cells from each well were harvested for aldosterone measurement and RNA extraction. Three

experiments using aldosterone secretagogues ($n=9$) and two experiments using calcium channel blockers ($n=6$) were independently conducted in triplicate.

Human ClC-2-targeting (TRCN0000427876) and non-mammalian control (SHC002V) MISSION shRNA lentiviral transduction particles were obtained from Sigma-Aldrich. The shRNA sequences were inserted into the TRC2 pLKO-puro plasmid backbone. For lentiviral infections, the manufacturer's protocol was followed with slight modifications. 1×10^4 H295R-S2 cells were seeded in a 96-well plate. After 24 h, medium was changed and supplemented with 2 µg/ml polybrene (Sigma). Lentiviral particles were then added at a multiplicity of infection of 10 and the medium was changed after overnight incubation. For selection, 2 µg/ml puromycin (Gibco) was added to the medium. After two passages, cells were characterized in terms of mRNA expression and aldosterone production after incubation with or without secretagogue as mentioned above.

RNA extraction and RT–qPCR. Total RNA was extracted in TRIzol reagent (Ambion, Life Technologies) according to the manufacturer's recommendations. After DNase I treatment (Life Technologies), 500 ng of total RNA was reverse transcribed (iScript reverse transcriptase, Bio-Rad). Primers used for qPCR are described in Supplementary Table 3. qPCR was performed using SYBR Green (Sso Advanced Universal SYBR Green Supermix, Bio-Rad) on a C1000 touch thermal cycler from Bio-Rad (CFX96 Real-Time System), according to the manufacturer's instructions. Controls without template were included to verify that fluorescence was not overestimated from primer-dimer formation or PCR contaminations. RT–qPCR products were analyzed in a postamplification fusion curve to ensure that a single amplicon was obtained. Normalization for RNA quantity and reverse transcriptase efficiency was performed against three reference genes (geometric mean of the expression of 18 S rRNA, *HPRT1*, and *GAPDH*), in accordance with the MIQE guidelines[42]. Quantification was performed using the standard curve method. Standard curves were generated using serial dilutions from a cDNA pool of all samples of each experiment, yielding a correlation coefficient of at least 0.98 in all experiments.

Aldosterone and protein assays. Aldosterone levels were measured in cell culture supernatants by ELISA. Antibody to aldosterone and aldosterone-3-CMO-biotin were kindly provided by C. Gomez-Sanchez[43]. Aldosterone concentrations were normalized to cell protein concentrations (determined using Bradford protein assays).

Statistical analyses. Quantitative variables are reported as means ± s.e.m. when a Gaussian distribution was present or as medians and interquartile ranges when no Gaussian distribution was present. Pairwise comparisons were done with unpaired *t* tests and Mann–Whitney tests, respectively; multiple comparisons were done with the ANOVA test followed by a test for pairwise comparison of subgroups according to Bonferroni when a Gaussian distribution was present or Kruskal–Wallis followed by Dunn's test when no Gaussian distribution was present. Comparisons between two groups were performed with two-tailed *t* tests or two-tailed Mann–Whitney tests. A P value of <0.05 was considered significant. For functional experiments, all results are expressed as means ± s.e.m. of three separate experiments performed in triplicate for ClC-2 overexpression studies with secretagogues, two separate experiments performed in triplicate for ClC-2 expression studies with calcium channel blockers, and two to four separate experiments performed in triplicate for ClC-2 knockdown studies. Analyses were performed using Prism5 (GraphPad).

URLs. Software used to analyze the whole-exome sequencing data, https://ihg4.helmholtz-muenchen.de/cgi-bin/mysql/snv-vcf/login.pl.

Life Sciences Reporting Summary. Further information on experimental design is available in the Life Sciences Reporting Summary.

Data availability. The data that support the findings of this study are available from the authors upon reasonable request; see author contributions for specific datasets. Disease-causing variants have been submitted to ClinVar. Exome data are available upon request within a scientific cooperation.

References

37. Hubert, E. L. et al. Mineralocorticoid receptor mutations and a severe recessive pseudohypoaldosteronism type 1. *J. Am. Soc. Nephrol.* **22**, 1997–2003 (2011).
38. Günther, W., Lüchow, A., Cluzeaud, F., Vandewalle, A. & Jentsch, T. J. ClC-5, the chloride channel mutated in Dent's disease, colocalizes with the proton pump in endocytotically active kidney cells. *Proc. Natl. Acad. Sci. USA* **95**, 8075–8080 (1998).
39. Gomez-Sanchez, C. E. et al. Development of monoclonal antibodies against human CYP11B1 and CYP11B2. *Mol. Cell. Endocrinol.* **383**, 111–117 (2014).
40. Hu, C., Rusin, C. G., Tan, Z., Guagliardo, N. A. & Barrett, P. Q. Zona glomerulosa cells of the mouse adrenal cortex are intrinsic electrical oscillators. *J. Clin. Invest.* **122**, 2046–2053 (2012).
41. Wang, T. et al. Comparison of aldosterone production among human adrenocortical cell lines. *Horm. Metab. Res.* **44**, 245–250 (2012).
42. Bustin, S. A. et al. The MIQE guidelines: minimum information for publication of quantitative real-time PCR experiments. *Clin. Chem.* **55**, 611–622 (2009).
43. Gomez-Sanchez, C. E. et al. The production of monoclonal antibodies against aldosterone. *Steroids* **49**, 581–587 (1987).

nature research

Corresponding author(s): Maria-Christina Zennaro, Fabio L Fernandes-Rosa, Thomas J Jentsch

☐ Initial submission ☐ Revised version ☒ Final submission

Life Sciences Reporting Summary

Nature Research wishes to improve the reproducibility of the work that we publish. This form is intended for publication with all accepted life science papers and provides structure for consistency and transparency in reporting. Every life science submission will use this form; some list items might not apply to an individual manuscript, but all fields must be completed for clarity.

For further information on the points included in this form, see Reporting Life Sciences Research. For further information on Nature Research policies, including our data availability policy, see Authors & Referees and the Editorial Policy Checklist.

Experimental design

1. Sample size

Describe how sample size was determined.

No sample-size calculation was performed. For functional experiments, two to three separate experiments were performed in experimental triplicates for ClC-2 overexpression studies and two to four separate experiments were performed in experimental triplicate for ClC-2 knockdown studies. This sample sizes are considered sufficient, given the inter- and intraexperimental variability observed in previous studies.

2. Data exclusions

Describe any data exclusions.

No data were excluded from the analysis.

3. Replication

Describe whether the experimental findings were reliably reproduced.

The experimental findings were reliably reproduced.

4. Randomization

Describe how samples/organisms/participants were allocated into experimental groups.

Randomization is not relevant to this study.

5. Blinding

Describe whether the investigators were blinded to group allocation during data collection and/or analysis.

Blinding was not relevant to this study.

Note: all studies involving animals and/or human research participants must disclose whether blinding and randomization were used.

6. Statistical parameters

For all figures and tables that use statistical methods, confirm that the following items are present in relevant figure legends (or in the Methods section if additional space is needed).

n/a	Confirmed
☐	☒ The exact sample size (*n*) for each experimental group/condition, given as a discrete number and unit of measurement (animals, litters, cultures, etc.)
☐	☒ A description of how samples were collected, noting whether measurements were taken from distinct samples or whether the same sample was measured repeatedly
☐	☒ A statement indicating how many times each experiment was replicated
☐	☒ The statistical test(s) used and whether they are one- or two-sided (note: only common tests should be described solely by name; more complex techniques should be described in the Methods section)
☐	☒ A description of any assumptions or corrections, such as an adjustment for multiple comparisons
☐	☒ The test results (e.g. *P* values) given as exact values whenever possible and with confidence intervals noted
☐	☒ A clear description of statistics including central tendency (e.g. median, mean) and variation (e.g. standard deviation, interquartile range)
☐	☒ Clearly defined error bars

See the web collection on statistics for biologists for further resources and guidance.

Software

Policy information about availability of computer code

7. Software

Describe the software used to analyze the data in this study.	Electrophysiological recordings were analyzed with Clampfit software 10.4. Statistical analyses were done the GraphPad Prism software

For manuscripts utilizing custom algorithms or software that are central to the paper but not yet described in the published literature, software must be made available to editors and reviewers upon request. We strongly encourage code deposition in a community repository (e.g. GitHub). *Nature Methods* guidance for providing algorithms and software for publication provides further information on this topic.

Materials and reagents

Policy information about availability of materials

8. Materials availability

Indicate whether there are restrictions on availability of unique materials or if these materials are only available for distribution by a for-profit company.	Small amounts of plasmids suitable for trasformation will be made available to other researchers. The self-made ClC-2 antibodies used in this study (already described in Hoegg-Beiler...Jentsch, NatureComm (2014) will be made available in reasonable quantities to other researchers, as already done previously. The ClC-2 KO mice (first described in Bösl...Jentsch, EMBO J (2001)) will also be made available to other researchers, as already done previously (see Speake...Brown, J Physiol (2002); and Makara...Kettenmann, MolCellNeurosci (2003)). This is contingent on the costs of shipment etc paid by the receiving lab, stating our help in the acknowledgement, and written assurance not to give the material out to others without our consent and not to use the material for commercial purposes. For mice, the receiving lab also has to give assurance that the animals will be kept and treated according to official regulations concerning animal welfare.

9. Antibodies

Describe the antibodies used and how they were validated for use in the system under study (i.e. assay and species).	Rabbit polyclonal antibodies against a modified carboxy-terminal ClC-2 peptide were used for Western blots. They have been previously described in Hoegg-Beiler, M.B. et al. Disrupting MLC1 and GlialCAM and ClC-2 interactions in leukodystrophy entails glial chloride channel dysfunction. Nat Commun 5, 3475 (2014). In that paper, their specificity was ascertained using tissue from our ClC-2 KO mice. Also in the present work, we have used adrenal glands from ClC-2 KO mice to ascertain their specificity (see Fig. 2a).

10. Eukaryotic cell lines

a. State the source of each eukaryotic cell line used.	The human adrenocortical carcinoma cell line H295R strain 2 (H295R-S2), kindly provided by W. E. Rainey, University of Michigan Ann Arbor, MI (Wang, T. et al. Comparison of aldosterone production among human adrenocortical cell lines. Horm Metab Res 44, 245-50 (2012).
b. Describe the method of cell line authentication used.	The adrenal cell lines used were authenticated by the measurement of aldosterone seceration and upregulation of mRNAs coding for steroidogenic enzymes in reponse to known stimuli of aldosterone secretion (AngII, K).
c. Report whether the cell lines were tested for mycoplasma contamination.	The cell lines tested negative for mycoplasma contamination.
d. If any of the cell lines used are listed in the database of commonly misidentified cell lines maintained by ICLAC, provide a scientific rationale for their use.	No commonly misidentified cell line was used.

Animals and human research participants

Policy information about studies involving animals; when reporting animal research, follow the ARRIVE guidelines

11. Description of research animals

Provide details on animals and/or animal-derived materials used in the study.

We used WT and Clcn2-/- mice (Mus musculus, C57/Bl6 genetic background) to obtain tissue for analysis by Western blotting and electrophysiology. The Clcn2-/- mice have been described before (Bösl...Jentsch, EMBO J. (2001)). Adult mice of both sexes were used. In detail: For the Western blot shown in Fig. 2a, the brain tissue was from a 30 week-old male WT mice; the adrenal glands from a 58 week-old male WT mice and from a 56 week-old male ClC-2 KO mice.
For the electrophysiological analysis of chloride currents in zona glomerulosa cells. the following mice were used: WT: 2 males and 1 female, between 4 and 7 weeks of age; KO: 2 females, 6 and 10 weeks of age.
Xenopus oocytes were taken from female Xenopus laevis frogs obtained from commercial suppliers by surgically removing the ovaries and isolating oocytes. These interventions and the keeping of Xenopus in our facility were according to German and European regulations and have been approved by the local authority (LAGeSo).
The keeping of mice in the animal facility of the MDC and the method of sacrificing them for taking tissues also conformed to German and European laws and were approved by LAGeSo. These procedures are not legally considered as animal experiments.

Policy information about studies involving human research participants

12. Description of human research participants

Describe the covariate-relevant population characteristics of the human research participants.

All relevant information on human research participants has been provided in the manuscript.